HHS Public Access

Author manuscript

FEMS Yeast Res. Author manuscript; available in PMC 2015 May 12.

Published in final edited form as:

FEMS Yeast Res. 2013 May ; 13(3): 302–311. doi:10.1111/1567-1364.12035.

Heterologous expression of *Candida albicans* Pma1p in *Saccharomyces cerevisiae*

Mikhail V. Keniya[1], **Richard D. Cannon**[1], **ẤnBình Nguyễn**[2], **Joel D. A. Tyndall**[2], and **Brian C. Monk**[1]

[1]The Sir John Walsh Research Institute, School of Dentistry, University of Otago, Dunedin, New Zealand [2]School of Pharmacy, University of Otago, Dunedin, New Zealand

Abstract

Candida albicans is a major cause of opportunistic and life-threatening systemic fungal infections, especially in the immunocompromised. The plasma membrane proton pumping ATPase (Pma1p) is an essential enzyme that generates the electrochemical gradient required for cell growth. We expressed *C. albicans* Pma1p (CaPma1p) in *Saccharomyces cerevisiae* to facilitate screening for inhibitors. Replacement of *S. cerevisiae PMA1* with *C. albicans PMA1* gave clones expressing CaPma1p that grew slowly at low pH. CaPma1p was expressed at significantly lower levels and had lower specific activity than the native Pma1p. It also conferred pH sensitivity, hygromycin B resistance and low levels of glucose-dependent proton pumping. Recombination between *CaPMA1* and the homologous non-essential *ScPMA2* resulted in chimeric suppressor mutants that expressed functional CaPma1p with improved H^+-ATPase activity and growth rates at low pH. Molecular models of suppressor mutants identified specific amino acids (between 531-595 in CaPma1p) that may affect regulation of the activity of Pma1p oligomers in *S. cerevisiae*. A modified CaPma1p chimeric construct containing only 5 amino acids from ScPma2p enabled the expression of a fully functional enzyme for drug screens and structural resolution.

Keywords

yeast; *PMA1*; plasma membrane H^+-ATPase; proton pump; antifungal drug target

Introduction

Candida albicans remains the dominant cause of both opportunistic and life-threatening systemic fungal infections, especially in the immunocompromised (Pfaller & Diekema, 2007). P-type ATPases are widely used as drug targets for specific interventions in a diverse range of human diseases (Yatime *et al.*, 2009). In fungi the plasma membrane proton pumping ATPase (Pma1p) is an essential enzyme that generates the electrochemical gradient required for nutrient uptake and ionic homeostasis (Serrano *et al.*, 1986). The synthesis of Pma1p is tightly transcriptionally regulated and its activity is controlled by pH and glucose

Correspondence: Mikhail V. Keniya, Department of Oral Sciences, School of Dentistry, University of Otago, PO Box 647, Dunedin 9054, New Zealand, Tel: +64 3 479 7080; Fax: +64 3 479 7078 mikhail.keniya@otago.ac.nz.

via phosphorylation of its C-terminal domain (Mason *et al.*, 1998, Martin-Castillo & Portillo, 1999, Lecchi *et al.*, 2007). Fungal P-type ATPases are sufficiently conserved within their membrane sector and ectodomain to provide a broad-spectrum antifungal target and differ enough from key human P-type ATPases to minimize the risk of host toxicity (Monk & Perlin, 1994). Fungal Pma1p has been validated as an antifungal drug target but has yet to provide drugs used in the clinic (Monk *et al.*, 1995, Perlin *et al.*, 1997, Monk *et al.*, 2005, Billack *et al.*, 2010). In addition, a structure of Pma1p from a yeast or fungal pathogen at a resolution that would aid drug discovery has yet to be determined.

Although the *Arabidopsis thaliana* AHA2 plasma membrane proton pump (Pedersen *et al.*, 2007) and human and rabbit Ca^{2+}-ATPase have been structurally resolved to 3.6 Å and 2.15 Å respectively (Toyoshima, 2008, Toyoshima *et al.*, 2011), the only structure available for a fungal P-type ATPase is a low resolution (8 Å) cryo-electron microscopy-based model of *Neurospora crassa* Pma1p (Auer *et al.*, 1998). We believe that the heterologous expression of *C. albicans* Pma1p (CaPma1p) in the model yeast *Saccharomyces cerevisiae* should enable new screens for Pma1p-specific inhibitors and structure-directed antifungal discovery by making cell growth dependent on the target enzyme and by producing homogeneous enzyme in the quantities needed for structural analysis. Our preliminary studies suggested that heterologous expression would be feasible (Mason *et al.*, 1996). We found that a chimeric *S. cerevisiae* Pma1p containing *C. albicans* transmembrane loops 1 + 2 and 3 + 4 gave growth rates, growth yields, glucose-dependent proton pumping rates, acid-activated omeprazole sensitivities, salt tolerances and antifungal sensitivities comparable to the parental *S. cerevisiae* enzyme. These experiments demonstrated cross-species complementarity for this combination of transmembrane loops. In contrast, single heterologous transmembrane loops caused deleterious phenotypes at either low pH or elevated temperature (Mason *et al.*, 1996). The compatibility of other parts of CaPma1p with the *S. cerevisiae* enzyme is not known. We have therefore explored the consequences of expressing *CaPMA1* in place of *ScPMA1* and identified structural features needed for Pma1p function.

Materials and methods

Yeast strains and yeast culture

The *S. cerevisiae* strains used in the study (Table 1) were grown in YPD medium (1% yeast extract, 2% peptone and 2% glucose). Synthetic complete supplement mixture (CSM, Formedia, UK) containing 10 mM MES and 20 mM HEPES buffered to the indicated pH with TRIS, either as a nutrient dropout, or supplemented with the indicated drug, was used for strain maintenance and selection of mutants. For liquid assays, buffered CSMYP media (CSM supplemented with 0.1% yeast extract, 0.2% peptone) allowed cultures to grow to higher cell densities. The haploid *S. cerevisiae* strain ADΔ (MMLY663, Table 1) used as an expression host (Lamping *et al.*, 2005, Lamping *et al.*, 2007) was derived from strain AD1-8u^{-} (Decottignies *et al.*, 1998).

Yeast constructs

Yeast were transformed using an Alkali-Cation transformation kit (Bio 101, Vista, CA USA). *S. cerevisiae* MMLY1019 (ADΔ, Δ*PMA2::kanMX4*) was derived from ADΔ by gene disruption using a cassette containing the recyclable kanMX4 marker flanked with loxP repeats and bordered with *ScPMA2*-specific arms (Guldener *et al.*, 1996). Transformants were selected on CSM media containing geneticin (200 μg mL^{-1} G418, Sigma). Transformation cassettes for *PMA1* replacement were created by fusion PCR using flanking primers, up to 4 DNA fragments containing 25-30 nucleotide overlaps and KOD Hot Start DNA Polymerase (Novagen®). The *CaPMA1* ORF was amplified from *C. albicans* SC5314. Plasmid pDP100 (Seto-Young *et al.*, 1994) was used as a template for the 584 bp fragment immediately upstream of the *ScPMA1* ORF and a 650 bp fragment immediately downstream of the ORF. The fragment containing the *S. cerevisiae PGK1* terminator plus the *S. cerevisiae URA3* gene was amplified using the pABC3 vector (Lamping *et al.*, 2007) as template. Transformants were selected on CSM-Ura dropout medium. The sequences of the ORFs, promoters and downstream sequences involved in strain construction were confirmed by DNA sequence analysis.

Hygromycin B resistance

Yeast cells (200 μL, OD_{600} = 0.2, 6×10^5 CFU) suspended in 5 mL of YPD containing 0.6% (w/v) agarose at 49°C were rapidly poured onto 20 mL of the same medium solidified in a petri dish. Six mm BBL™ paper disks containing 400 nmole of hygromycin B were applied to the set agarose surface. The plates were incubated at 30°C for 48 h and the diameters of the growth inhibition zones (W) were measured. Relative hygromycin B resistance was calculated as $W_{(AD\ \Delta)}/W_{(strain\ x)}$.

Acid resistance

CSMYP media was adjusted with either TRIS or HCl to the indicated pH between 3.0 and 7.5. The medium (200 μL final volume per well) in 96 well microtitre plates was inoculated with cells in late logarithmic phase to OD_{600} = 0.08. The optical densities of the cultures were recorded after 24 h incubation at 30°C with shaking (150 rpm) using an EL-340 microplate reader (Bio-Tek™). A final cell density of OD_{600} ~ 1.2 indicated optimal growth.

Glucose-dependent proton pumping

The acidification of the media caused by glucose-dependent H^+-ATPase activity in live cells was evaluated as described previously (Monk *et al.*, 2005). In brief, cells grown in CSM at pH 6.5 to mid-log phase (OD_{600} ~3) were washed and starved overnight in distilled water on ice. A microtitre plate assay of glucose-dependent proton pumping was performed using replicate samples at 30°C, with the pH of the reaction mixture pre-adjusted to 5.0 with HCl. The incubation pre-mix (150 μL) contained 50 μL each of yeast cell suspension at OD_{600} = 16, bromophenol blue at 140 μg mL^{-1}, and either water or 200 mM KCl. After equilibration to room temperature (21°C), the reaction was initiated by adding 50 μL of 8% D-glucose. The OD_{590} was measured at 33 s intervals for 40 min using a Synergy 2 microplate reader (BioTek™), with the plate shaken prior to each measurement. The absorbance of

bromophenol dye at 590 nm was used to monitor the pH between 5.0 and 3.5. The maximum rate (MaxV) of glucose-dependent proton pumping was determined using Gen5 software (BioTek™).

Plasma membrane preparation and analysis

Yeast cells were grown to early diauxic phase (OD_{600} = 5-5.5) in CSMYP containing 10 mM MES-HEPES adjusted with TRIS to pH 7.0. Harvested cells were resuspended (60-70 OD_{600} mL^{-1}) in ice-cold homogenizing medium (20% (w/v) glycerol, 0.5 mM EDTA, 1 mM PMSF 50 mM TRIS pH 7.5) containing 100 mM glucose. After incubation for 1 h at 4°C, the pH was adjusted to 7.5 and the cells homogenized using a Beadbeater™ (BioSpec Products Inc, Bartlesville, OK, USA). Crude membranes were pelleted by differential centrifugation and an enriched plasma membrane preparation was obtained after acid precipitation (Goffeau & Dufour, 1988). Protein concentration was estimated using the Bradford assay (Bio-Rad, Richmond, CA, USA) with bovine IgG as standard. Plasma membranes dissolved at room temperature in SDS-lysis buffer (2% SDS, 50 mM Tris-HC1 pH 6.7, 10% glycerol, 2.5 mM EDTA, 0.01% PMSF, 1 μg mL^{-1} bromophenol blue, 40 mM dithiothreitol) were separated by SDS-PAGE (Laemmli, 1970). The photographic images of the gels were analysed for Pma1p band density relative to the whole line using UN-SCAN-IT gel™ V.6.1 software (Silk Scientific Corporation). Protein bands excised from Coomassie R250-stained polyacrylamide gels were analysed by MALDI-TOF mass spectrometry of tryptic fingerprints at the Centre for Protein Research of the University of Otago.

Preparation of Pma1p

Plasma membrane samples (1 mg mL^{-1}) were treated with deoxycholate (DOC; 5 mg mL^{-1}) in the presence of soy phosphatidylcholine (1 mg mL^{-1}, Sigma) at pH 7.2 for 10 min on ice and the stripped membranes pelleted at ~92,000 g for 45 min. The stripped membranes (0.5 mg mL^{-1}) were solubilized in 2mM (5× CMC) of Zwittergent 3-14 (SB3-14, Sigma) at pH 6.5 in the presence of bovine brain lipid extract (6 mg mL^{-1}, Folch fraction III, Sigma). The solubilised Pma1p-containing vesicles were pelleted at 308,000 g for 16 h and excess lipid removed by washing with the Zwittergent 3-14-containing buffer.

Size exclusion chromatography

Zwittergent-washed Pma1p-enriched samples were separated by size exclusion chromatography using a Superdex 200 10/300 (GE Healthcare) column on an ÄCTA™ FPLC system at a flow rate of 0.5 mL min^{-1}. The buffer contained 4mM (10× CMC) Zwittergent 3-14, 0.2 M KCl, 0.3 M NaCl, 0.5 mM PMSF, 1 tablet of Complete Mini EDTA-free protease inhibitor cocktail (Roche, USA) per 100 ml, in 10 mM HEPES-HCl pH 7.2. Fractions recovered at an elution volume comparable to the ferritin standard (~440 kDa) were pooled, precipitated using ice-cold 80% acetone and analysed by SDS-PAGE with silver staining (Merril *et al.*, 1981). The PageRuler™ Prestained Protein Ladder Plus (Fermentas) was used as a molecular weight standard.

Pma1p ATPase activity

The ATPase activity and kinetic parameters (K_m and V_{max}) of Pma1p in enriched plasma membrane preparations were measured as previously described (Monk *et al.*, 1991) as vanadate (100 μM) sensitive and oligomycin (20 μM) insensitive phosphate release from 15 mM Mg-ATP at pH 6.5 and 7.5 at 30°C

Homology modeling

Homology models of CaPma1p and ScPma1p were generated using Modeller 9v9 (Eswar *et al.*, 2006) using the known structure of the P-type H^+ ATPase from *A. thaliana* (PDB ID: 3B8C) (Pedersen *et al.*, 2007) as a template. Sequence alignments between the yeast proteins and the template were carried out using T-coffee (Poirot *et al.*, 2003). Structural figures were prepared using PyMOL (The PyMOL Molecular Graphics System, Version 1.5.0.4 Schrödinger, LLC).

Results and Discussion

Expression of CaPma1p in S. cerevisiae

The *S. cerevisiae* strain ADΔ was chosen as an expression host for *C. albicans* Pma1p because it lacks 7 ABC-type transporters responsible for the efflux of a wide range of xenobiotics. The absence of these transporters was expected to provide enhanced xenobiotic sensitivity during cell-based inhibitor screening, decrease the background of ATPase activities during *in vitro* drug screens for Pma1p inhibition, and minimize membrane protein contamination during isolation of Pma1p. Heterologous expression of CaPma1p in *S. cerevisiae* ADΔ gave a ~100 kDa band visualized by Coomassie staining of SDS-PAGE separated, deoxycholate-extracted plasma membrane fractions (Fig. 1 A). ScPma1p from MMLY1019 had a slightly lower mobility (99.6 kDa) than both CaPma1p (97.5 kDa) extracted from *C. albicans* SC5314 and CaPma1p heterologously expressed in *S. cerevisiae* MMLY1021 (97.7 kDa). The Pma1p from MMLY1021 was found to be a chimera of CaPma1p and ScPma2p, as described below. The identities of the heterologously expressed Pma1ps were confirmed using MALDI-TOF mass spectrometry of the trypsin digested ~100 kDa bands excised from the gels after SDS-PAGE (data not shown).

Pma1p migrates as a multimer in size exclusion chromatography

Size exclusion chromatography in Zwittergent 3-14 showed that the three samples obtained from DOC-stripped *S. cerevisiae* plasma membranes by detergent extraction and washing gave broad peaks with mobilities comparable to ferritin (440 kDa; Fig. 2) which corresponded to at least a tetrameric complex of Pma1p monomers. A peak corresponding to the predicted Pma1p monomer (100 kDa, elution volume ~ 12-13 ml) was not detected. Bands which matched the expected sizes of the H^+-ATPase monomers were detected in silver stained polyacrylamide gels of the Superdex 200 fractions that eluted at 10.5-11.5 mL (Fig. 1 B).

Growth characteristics, hygromycin resistance and glucose-dependent proton pumping

At pH 6.0 ± 0.5 the *S. cerevisiae* ADΔ strain expressing CaPma1p (MMLY1022) had growth rates comparable to ADΔ. In unbuffered YPD or unbuffered CSM agar the CaPma1p expressing strain showed acid-sensitive growth and gave smaller colonies than the unmodified *S. cerevisiae* strain. Expression of the *Nicotiana plumbaginifolia PMA2* gene in *S. cerevisiae* gave a similar pH-sensitive phenotype (de Kerchove d'Exaerde *et al.*, 1995). The pH sensitivity of the CaPma1p-expressing strains correlated with modest expression of CaPma1p in plasma membrane fractions detected by SDS-PAGE, low ATPase activity *in vitro*, and increased resistance to hygromycin B compared to the ADΔ strain (Table 2). Uptake of the protein synthesis inhibitor hygromycin B and the size of the resultant growth inhibition zones in agarose diffusion assays depend on the electrogenic activity of Pma1p. The increased resistance of *S. cerevisiae* strains expressing CaPma1p to hygromycin B indicated reduced plasma membrane ATPase function (Table 2).

These results were confirmed by an *in vivo* ATPase assay measured as glucose-dependent proton efflux. Cells expressing CaPma1p acidified the medium at rates that were ~3 times lower than the control strain expressing ScPma1p (ADΔ) (Fig. 3). For ADΔ, inclusion of 200 mM KCl in the assay abolished the membrane potential of the plasma membrane and doubled the net rate of glucose-dependent proton pumping. The strain expressing CaPma1p was only half as responsive to the addition of 200 mM KCl, confirming the limited capacity of these cells to produce an electrochemical gradient.

Suppressor mutations resulting from recombination with PMA2

Suppressor mutants of MMLY1020, (MMLY1021 and MMLY1087) that showed enhanced growth rates at low pH, reduced resistance to hygromycin B and KCl-stimulated glucose-dependent proton pumping rates closer to the native ScPma1p in ADΔ were readily obtained as bigger colonies after overnight culture in YPD. DNA sequence analysis of the Pma1p ORF from these mutants revealed multiple recombination events between *CaPMA1* and *ScPMA2* (Table 2). *ScPMA2* is a non-essential homologue of *ScPMA1* (Supplementary Table S1, Fig. S1) that is weakly expressed under normal culture conditions (Supply *et al.*, 1993). ScPma2p expressed under the control of the *PMA1* promoter was found to partially complement the essential activity of ScPma1p but some acid sensitivity remained. A similar phenomenon of compensatory recombination was encountered during heterologous expression of the *N. plumbaginifolia PMA* gene in *S. cerevisiae* (Harris *et al.*, 1994, de Kerchove d'Exaerde *et al.*, 1995).

DNA sequence alignment showed that all *CaPMA1* suppressor isolates obtained in the present study had substitutions from *ScPMA2* between nucleotides 1521-1821 of *CaPMA1*. These resulted in up to 9 amino acid changes in two groups (Group 1 and Group 2) within a region of 32 amino acid residues in the CaPma1p primary sequence located in the C-terminal part of phosphorylation domain, according to AHA2 model alignment (Pedersen *et al.*, 2007) Strain MMLY1021 had an additional V186I substitution in actuator domain sequence. Chimeric strain MMLY1087 had the least number of amino acid replacements, with 5 ScPma2p-specific substitutions between amino acids 570-601 of CaPma1p i.e. it was CaPma1p apart from 5 amino acids in C-terminal part of phosphorylation domain, which

came from *ScPMA2* (Table 2, Supplementary Fig. S1). The amino acid substitutions were identical in ScPma1p and ScPma2p. These changes restored wild type resistance to acidic media and gave increased susceptibility to hygromycin B. *In vitro* ATPase activity and the enzyme Vmax in enriched plasma membrane fractions increased >3-fold to ~1/3 of the value for CaPma1p from *C albicans* (Fig. 4, Supplementary Table S2). The relative contribution of ~100kDa Pma1p band to all preparations was in the range of 10-15%. The heterologously expressed unmodified CaPma1p showing the lowest level of correctly trafficked ATPase (10 %), the chimeras showing intermediate levels (12-13%) and the native enzymes the highest levels (14-15%). The ATPase activity of chimeric ATPase from MMLY1021 remained low despite five additional amino-acid substitutions. The low ATPase activity of MMLY1021 was consistent with the higher hygromycin resistance of this construct.

Homology modeling of CaPma1p and CaPma1p-ScPma2p chimeras

Detergent-extracted ScPma1p and CaPma1p appear to migrate as a multimer during size exclusion chromatography and ScPma1p has been detected as functional >400 kDa oligomers in lipid rafts (Bagnat *et al.*, 2001). Few crystal structures of P-type ATPases are available and modelling the multmeric forms of ScPma1p or CaPma1p is a challenge. Cryo-electron microscopy of purified *Neurospora crassa* Pma1p showed it to be a hexamer (Auer *et al.*, 1998) but the structure (PDB ID: 1MHS) is only at 8 Å resolution. Higher resolution structures are available for P-type ATPases from other kingdoms (< 3.6 Å for *A. thaliana* AHA2 and 2.15 Å for *Oryctolagus cuniculus* SERCA1a) but these have significantly lower homology with the fungal Pma1ps and have substantially different C-terminal domains. Homology models of ScPma1p and CaPma1p, based on the crystal structure of AHA2, indicate that the residues E596, R617 and N624 in ScPma1p and the homologous residues E573, N594 and S601 in CaPma1p are exposed to the surface of a cytoplasmic domain (Fig. 5). Although ScPma1p E596 and CaPma1p E573 are conserved, the surface orientation of this glutamate may be affected by steric clashes with the nearby Group 1 residues P593 and L597 in ScPma1p and the corresponding A570 and I574 in CaPma1p. Although the low resolution of NcPma1p structure does not enable visualisation of changing monomer-monomer interactions during the reaction cycle or due to regulatory modification, the model confirms that the corresponding *N. crassa* Pma1p residues E596, N617 and Q624 lie at the interface between subunits of a hexamer (Fig. 6, Supplementary Fig. S2). It also shows that the two *N. crassa* amino acid residues (N617 and Q624) with homology to the Group 2 chimeric substitutions are in close proximity of the Group 2R C-terminal domain amino acids 893-905 of an adjacent monomer. The group 2R region contains charged and polar residues and a conserved glutamate (E903 in NcPma1p, E901 in ScPma1p) that is part of a phosphorylation recognition site that regulates the kinetic properties and turnover of ATPase (Mason *et al.*, 1998, Mason *et al.*, 2006). Furthermore, an 18 amino acid C-terminal deletion of ScPma1p (E901 replaced with a stop codon) allowed the ATPase to be properly presented in the plasma membrane and retain full activity, while a 38 amino acid truncation (removing the entire group 2R residues) was mistrafficked and extensively degraded (Mason *et al.*, 2006). Thus the C-terminal domain after transmembrane segment 10 regulates ATPase turnover and activity. Our results therefore suggest that the residues involved in intermolecular contacts between the subunits of CaPma1p may have poor compatibility with functional expression in *S. cerevisiae* at low pH, resulting in modified enzyme activity,

inappropriate regulation, and protein mislocalization or enhanced degradation (Chang & Slayman, 1991).

Improved functional expression of CaPma1p in S. cerevisiae

In order to heterologously express CaPma1p in *S. cerevisiae* without recombination with *ScPMA2*, the *CaPMA1-URA3* cassette obtained by PCR from strain MMLY1020 or the chimeric cassette from strain MMLY1021 was used to transform strain ADΔ Δ*PMA2* (MMLY1019) to Ura^+. The growth rates, acid tolerance, hygromycin B resistance, Pma1p expression, and glucose-dependent proton pumping of the transformants were similar to that of their donor strain and, as expected, no suppressor mutants were obtained (data not shown). The properties of N-terminal hexahistidine tagged and non-tagged variants were similar (data not shown). This observation will assist future structure-function studies.

H^+-ATPase activities of yeast strains

All tested forms of Pma1p were vanadate sensitive with IC_{50}s 2-9μM (Supplementary Table S2). Measurement of the vanadate-sensitive and oligomycin-insensitive H^+-ATPase activities of enriched membrane fractions at pH 6.5 (Fig. 4) showed ScPma1p from *S. cerevisiae* ADΔ had significantly lower ATPase activity than the enzyme from wild-type *S. cerevisiae* strain SH122 (de Kerchove d'Exaerde *et al.*, 1995, Mason *et al.*, 1998). This may be due to a D718N mutation in the conserved ^{714}DNSLDID^{720} motif between transmembrane segments 5 and 6 of ADΔ Pma1p. Homology modeling suggests that this mutation lies in a groove at the extracellular vestibule of the proton pore. CaPma1p expressed in *S. cerevisiae* MMLY1022 had a significantly lower plasma membrane H^+-ATPase activity than CaPma1p obtained directly from *C. albicans* (Fig. 4, Supplementary Table S2). All recombinant strains tested, which expressed native and chimeric CaPma1p showed an elevated activity at pH 7.5 closer to the optimum obtained for native CaPma1p (Mason *et al.*, 1996). These results are consistent with the proton pumping assays described in Figure 3 except for the MMLY1021 preparation, which may not be stable to membrane purification and/or assay despite Pma1p being detected in high levels in membrane preparations (Fig. 4).

Post-translational C-terminal regulation strongly affects ScPma1p activity and turnover (Monk *et al.*, 1991, Mason *et al.*, 1998). Glucose metabolism and/or acidification of the cytosol (Eraso & Gancedo, 1987) trigger phosphorylation of residue S899 in *S. cerevisiae* Pma1p, giving a decreased K_m and an increased V_{max} (Eraso & Portillo, 1994). Phosphorylation of other C-terminal residues (E901, S911, T912) may also be involved in Pma1p regulation (Mason *et al.*, 1996, Lecchi *et al.*, 2007). Deletion of the C-terminus (ΔE901-918) locks the enzyme in an active state (Mason *et al.*, 1998). We hypothesize that Group 1 and Group 2 residues in CaPma1p provide a pH-sensitive platform that promotes blockage of the active site at low pH by the C-terminal domain. We propose that this causes inappropriate regulation of CaPma1p when it is heterologously expressed in *S. cerevisiae*. The incorporation of two groups of Pma2p residues allows the chimeric enzyme to work more efficiently than CaPma1p at low pH because the stringency of C-terminal regulation has been reduced. The conformation of the chimeras might also reduce mistrafficking and enzyme turnover.

Conclusion

CaPma1p expressed in *S.cerevisiae* partially complements the function of the essential, native enzyme ScPma1p at neutral pH. The recombinant enzyme causes acid-sensitive growth and hygromycin B resistance characteristic of limited proton pumping activity. These effects were moderated by recombination with *PMA2*, giving rise to CaPma1p-ScPma2p chimeras which minimally contain 5 amino acid substitutions that are conserved in ScPma1p and ScPma2p. Differences between native ScPma1p, heterologously expressed CaPma1p or CaPma1p-ScPma2p chimeras did not affect oligomerization of these enzymes. The structural location of the suppressor mutations in the chimeras and the biochemical properties of these enzymes suggest a role for localized interactions with the negative regulatory C-terminal domain near a key phosphorylation site. The phenotypic effects of these interactions may be overcome by simply removing the C-terminal regulatory domain (Mason *et al.*, 1998). With these insights, we anticipate the design of yeast strains expressing CaPma1p that will provide tools for targeted antifungal screens. In addition, the overexpression of a suitable hexahistidine-tagged CaPma1p-ScPma2p chimera in *S. cerevisiae* may enable large-scale production of the homogenous enzyme for *in vitro* assays and structural analysis.

Supplementary Material

Refer to Web version on PubMed Central for supplementary material.

Acknowledgements

This research was supported by NIH grants DE015075 and DE016885, and the NZ Lottery Grants Board.

References

Auer M, Scarborough GA, Kuhlbrandt W. Three-dimensional map of the plasma membrane H^+-ATPase in the open conformation. Nature. 1998; 392:840–843. [PubMed: 9572146]

Bagnat M, Chang A, Simons K. Plasma membrane proton ATPase Pma1p requires raft association for surface delivery in yeast. Mol Biol Cell. 2001; 12:4129–4138. [PubMed: 11739806]

Billack B, Pietka-Ottlik M, Santoro M, Nicholson S, Mlochowski J, Lau-Cam C. Evaluation of the antifungal and plasma membrane H^+-ATPase inhibitory action of ebselen and two ebselen analogs in *S. cerevisiae* cultures. J Enzyme Inhib Med Chem. 2010; 25:312–317. [PubMed: 20210698]

Chang A, Slayman CW. Maturation of the yeast plasma membrane H^+-ATPase involves phosphorylation during intracellular transport. J Cell Biol. 1991; 115:289–295. [PubMed: 1833410]

de Kerchove d'Exaerde A, Supply P, Dufour JP, Bogaerts P, Thines D, Goffeau A, Boutry M. Functional complementation of a null mutation of the yeast *Saccharomyces cerevisiae* plasma membrane H^+-ATPase by a plant H^+-ATPase gene. J Biol Chem. 1995; 270:23828–23837. [PubMed: 7559560]

Decottignies A, Grant AM, Nichols JW, de Wet H, McIntosh DB, Goffeau A. ATPase and multidrug transport activities of the overexpressed yeast ABC protein Yor1p. J Biol Chem. 1998; 273:12612–12622. [PubMed: 9575223]

Eraso P, Gancedo C. Activation of yeast plasma membrane ATPase by acid pH during growth. FEBS Lett. 1987; 224:187–192. [PubMed: 2960558]

Eraso P, Portillo F. Molecular mechanism of regulation of yeast plasma membrane H^+-ATPase by glucose. Interaction between domains and identification of new regulatory sites. J Biol Chem. 1994; 269:10393–10399. [PubMed: 8144622]

Eswar N, Webb B, Marti-Renom MA, Madhusudhan MS, Eramian D, Shen MY, Pieper U, Sali A. Comparative protein structure modeling using Modeller. Curr Protoc Bioinformatics. 2006 Chapter 5: Unit 5 6.

Goffeau A, Dufour JP. Plasma membrane ATPase from the yeast *Saccharomyces cerevisiae*. Methods Enzymol. 1988; 157:528–533. [PubMed: 2906716]

Guldener U, Heck S, Fielder T, Beinhauer J, Hegemann JH. A new efficient gene disruption cassette for repeated use in budding yeast. Nucleic Acids Res. 1996; 24:2519–2524. [PubMed: 8692690]

Harris SL, Na S, Zhu X, Seto-Young D, Perlin DS, Teem JH, Haber JE. Dominant lethal mutations in the plasma membrane H^+-ATPase gene of *Saccharomyces cerevisiae*. P Natl Acad Sci USA. 1994; 91:10531–10535.

Laemmli UK. Cleavage of structural proteins during the assembly of the head of bacteriophage T4. Nature. 1970; 227:680–685. [PubMed: 5432063]

Lamping E, Tanabe K, Niimi M, Uehara Y, Monk BC, Cannon RD. Characterization of the *Saccharomyces cerevisiae sec6-4* mutation and tools to create S. cerevisiae strains containing the *sec6-4* allele. Gene. 2005; 361:57–66. [PubMed: 16185821]

Lamping E, Monk BC, Niimi K, Holmes AR, Tsao S, Tanabe K, Niimi M, Uehara Y, Cannon RD. Characterization of three classes of membrane proteins involved in fungal azole resistance by functional hyperexpression in *Saccharomyces cerevisiae*. Eukaryot Cell. 2007; 6:1150–1165. [PubMed: 17513564]

Lecchi S, Nelson CJ, Allen KE, Swaney DL, Thompson KL, Coon JJ, Sussman MR, Slayman CW. Tandem phosphorylation of Ser-911 and Thr-912 at the C terminus of yeast plasma membrane H^+-ATPase leads to glucose-dependent activation. J Biol Chem. 2007; 282:35471–35481. [PubMed: 17932035]

Martin-Castillo B, Portillo F. Characterization of non-dominant lethal mutations in the yeast plasma membrane H^+-ATPase gene. Biochim Biophys Acta. 1999; 1417:32–36. [PubMed: 10076033]

Mason AB, Kardos TB, Monk BC. Regulation and pH-dependent expression of a bilaterally truncated yeast plasma membrane H^+-ATPase. Biochim Biophys Acta. 1998; 1372:261–271. [PubMed: 9675306]

Mason AB, Allen KE, Slayman CW. Effects of C-terminal truncations on trafficking of the yeast plasma membrane H^+-ATPase. J Biol Chem. 2006; 281:23887–23898. [PubMed: 16751629]

Mason AB, Kardos TB, Perlin DS, Monk BC. Functional complementation between transmembrane loops of *Saccharomyces cerevisiae* and *Candida albicans* plasma membrane H^+-ATPases. Biochim Biophys Acta. 1996; 1284:181–190. [PubMed: 8914582]

Merril CR, Dunau ML, Goldman D. A rapid sensitive silver stain for polypeptides in polyacrylamide gels. Anal Biochem. 1981; 110:201–207. [PubMed: 6163373]

Monk BC, Perlin DS. Fungal plasma membrane proton pumps as promising new antifungal targets. Crit Rev Microbiol. 1994; 20:209–223. [PubMed: 7802957]

Monk BC, Kurtz MB, Marrinan JA, Perlin DS. Cloning and characterization of the plasma membrane H^+-ATPase from *Candida albicans*. J Bacteriol. 1991; 173:6826–6836. [PubMed: 1834633]

Monk BC, Mason AB, Kardos TB, Perlin DS. Targeting the fungal plasma membrane proton pump. Acta Biochim Pol. 1995; 42:481–496. [PubMed: 8852338]

Monk BC, Montesinos C, Ferguson C, Leonard K, Serrano R. Immunological approaches to the transmembrane topology and conformational changes of the carboxyl-terminal regulatory domain of yeast plasma membrane H^+-ATPase. J Biol Chem. 1991; 266:18097–18103. [PubMed: 1833392]

Monk BC, Niimi K, Lin S, Knight A, Kardos TB, Cannon RD, Parshot R, King A, Lun D, Harding DR. Surface-active fungicidal D-peptide inhibitors of the plasma membrane proton pump that block azole resistance. Antimicrob Agents Chemother. 2005; 49:57–70. [PubMed: 15616276]

Pedersen BP, Buch-Pedersen MJ, Morth JP, Palmgren MG, Nissen P. Crystal structure of the plasma membrane proton pump. Nature. 2007; 450:1111–1114. [PubMed: 18075595]

Perlin DS, Seto-Young D, Monk BC. The plasma membrane H^+-ATPase of fungi. A candidate drug target? Ann NY Acad Sci. 1997; 834:609–617. [PubMed: 9405872]

Pfaller MA, Diekema DJ. Epidemiology of invasive candidiasis: a persistent public health problem. Clin Microbiol Rev. 2007; 20:133–163. [PubMed: 17223626]

Poirot O, O'Toole E, Notredame C. Tcoffee@igs: A web server for computing, evaluating and combining multiple sequence alignments. Nucleic Acids Res. 2003; 31:3503–3506. [PubMed: 12824354]

Serrano R, Kielland-Brandt MC, Fink GR. Yeast plasma membrane ATPase is essential for growth and has homology with (Na^+ + K^+), K^+- and Ca^{2+}-ATPases. Nature. 1986; 319:689–693. [PubMed: 3005867]

Seto-Young D, Na S, Monk BC, Haber JE, Perlin DS. Mutational analysis of the first extracellular loop region of the H^+-ATPase from *Saccharomyces cerevisiae*. J Biol Chem. 1994; 269:23988–23995. [PubMed: 7929048]

Supply P, Wach A, Thines-Sempoux D, Goffeau A. Proliferation of intracellular structures upon overexpression of the PMA2 ATPase in *Saccharomyces cerevisiae*. J Biol Chem. 1993; 268:19744–19752. [PubMed: 8366114]

Toyoshima C. Structural aspects of ion pumping by Ca^{2+}-ATPase of sarcoplasmic reticulum. Arch Biochem Biophys. 2008; 476:3–11. [PubMed: 18455499]

Toyoshima C, Yonekura S, Tsueda J, Iwasawa S. Trinitrophenyl derivatives bind differently from parent adenine nucleotides to Ca^{2+}-ATPase in the absence of Ca^{2+} P Natl Acad Sci USA. 2011; 108:1833–1838.

Yatime L, Buch-Pedersen MJ, Musgaard M, et al. P-type ATPases as drug targets: tools for medicine and science. Biochim Biophys Acta. 2009; 1787:207–220. [PubMed: 19388138]

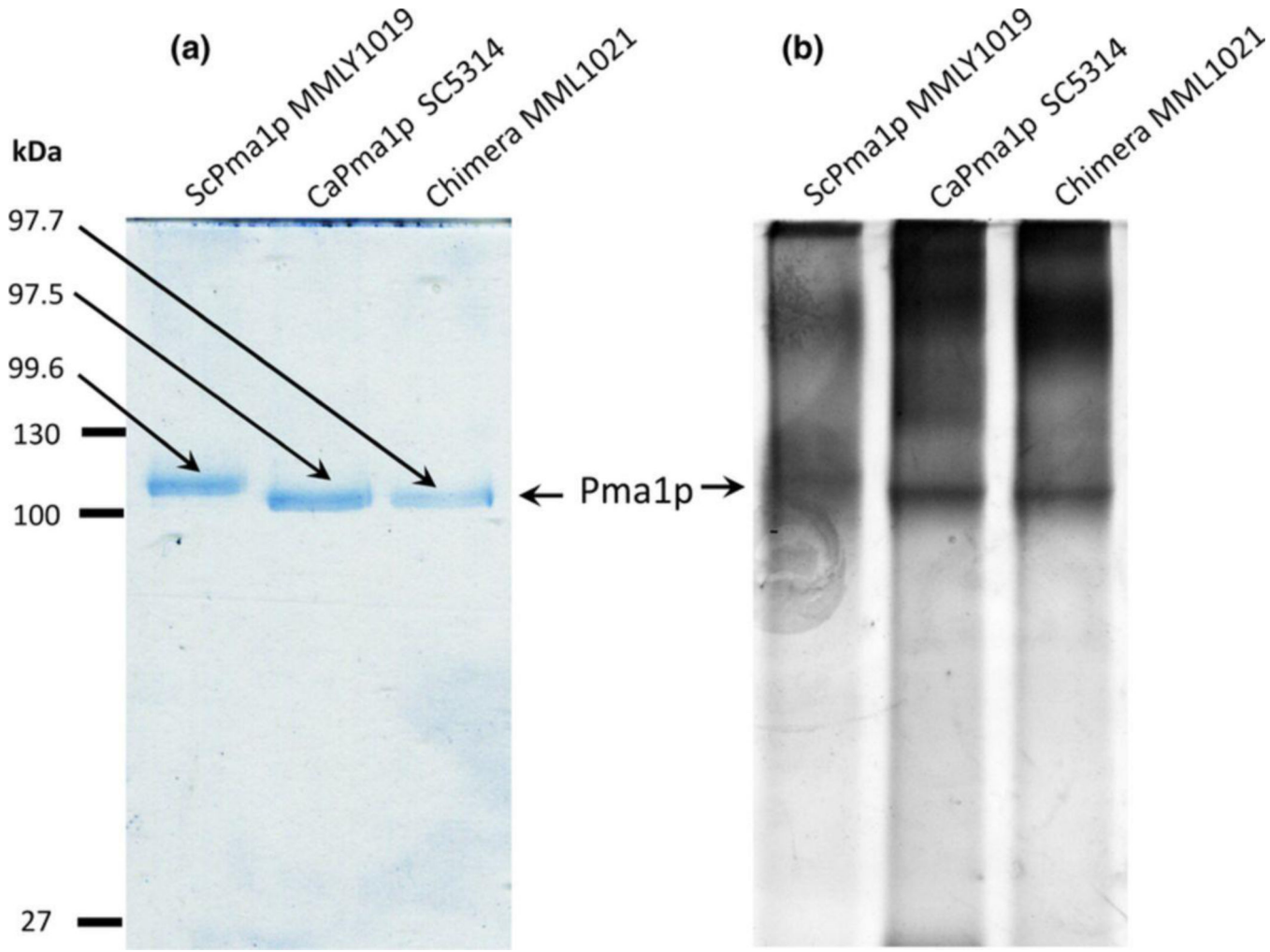

Figure 1.
SDS-PAGE analysis/gel of purified Pma1p.

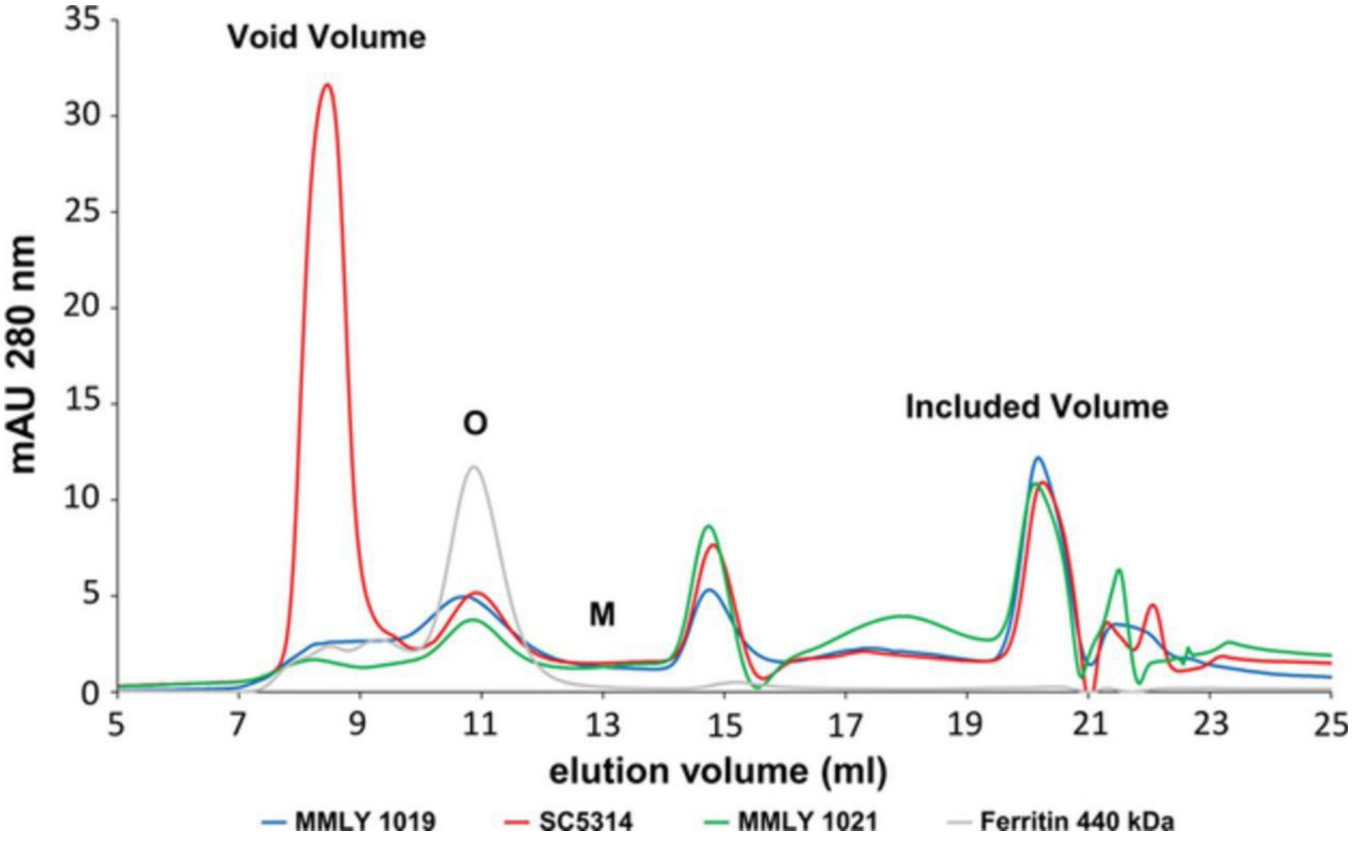

Figure 2.
Oligomeric Pma1p is observed during size exclusion chromatography.

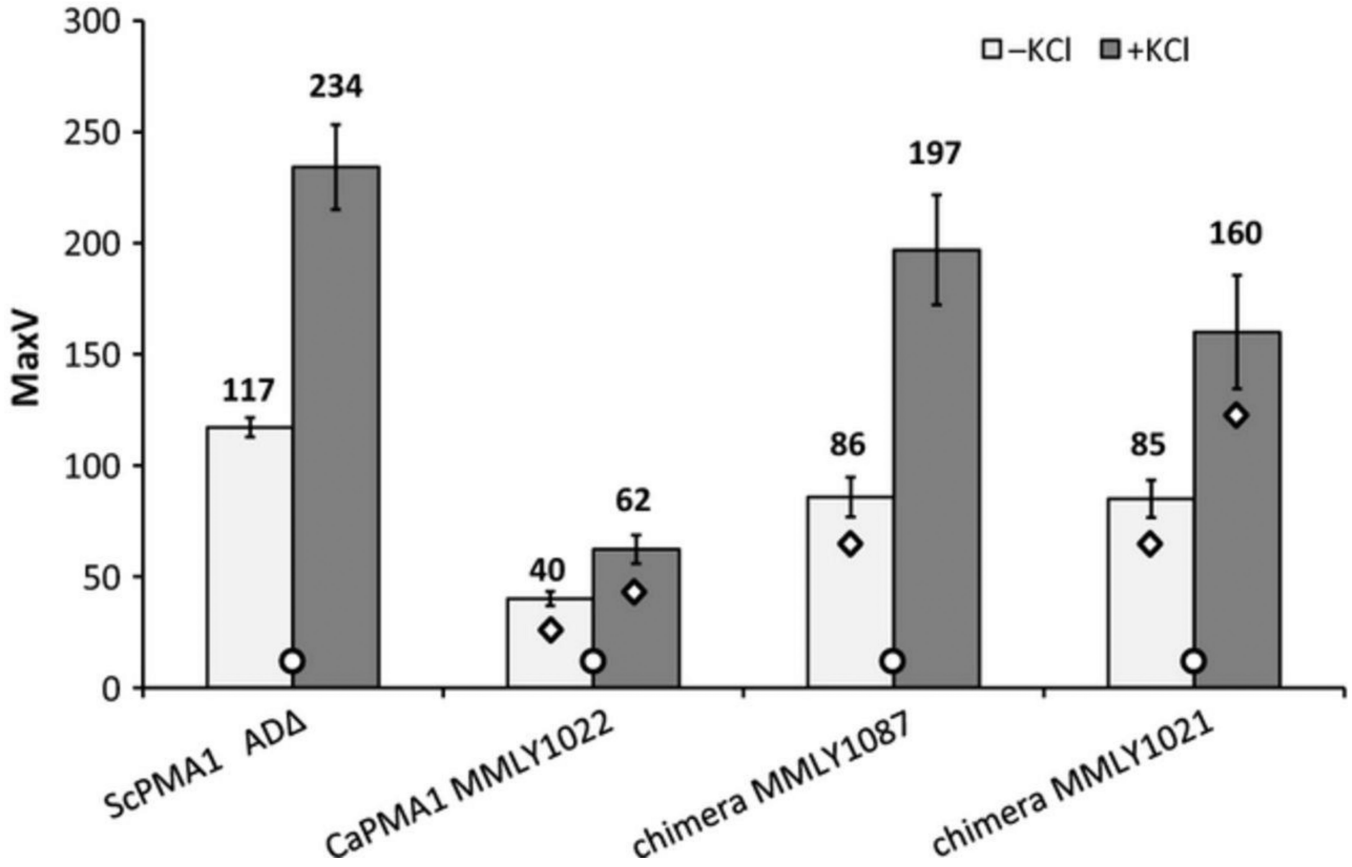

Figure 3.
Pma1p-mediated proton pumping activity.

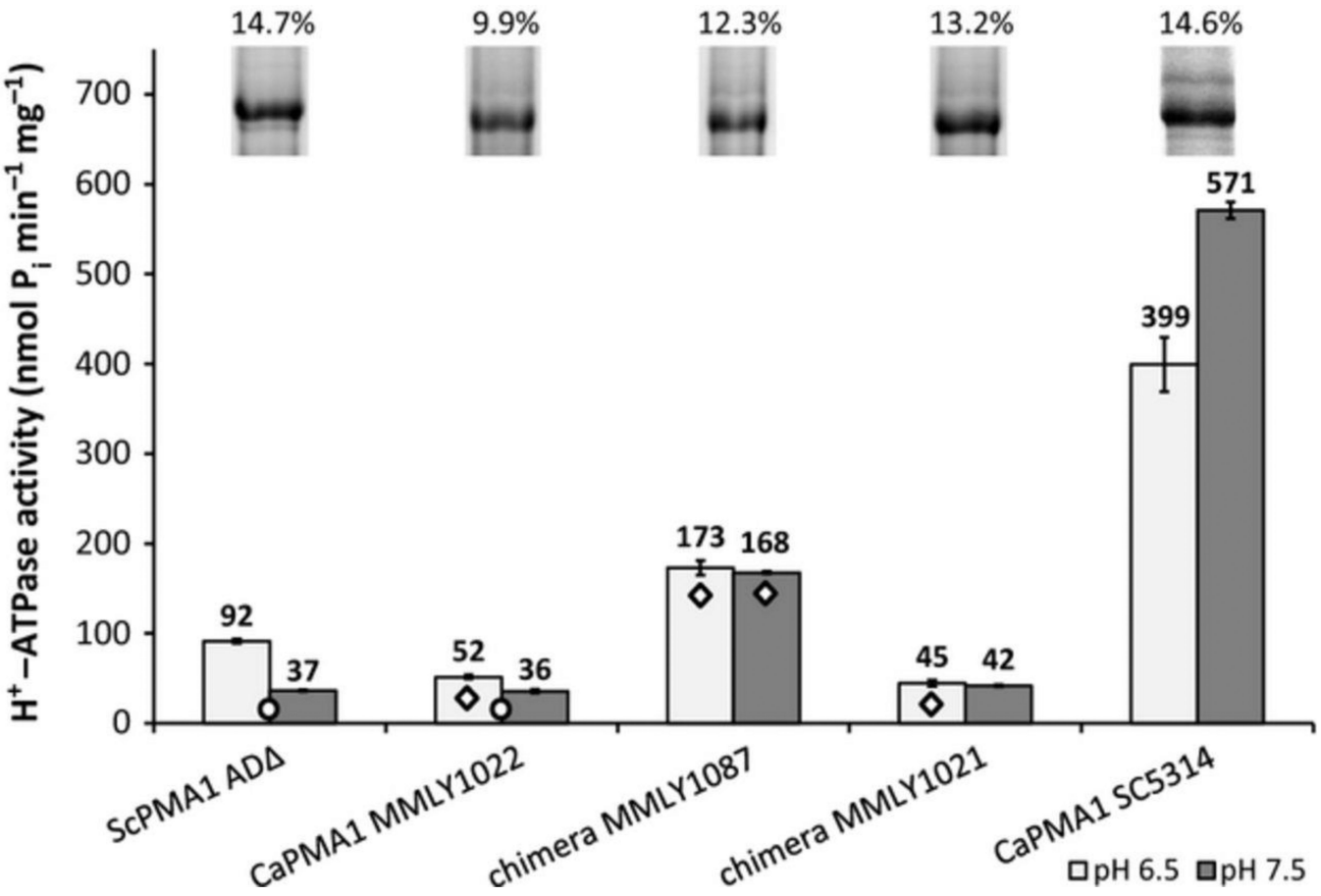

Figure 4.

Relative content and ATPase activities of Pma1p in enriched membrane fractions of yeast at pH 6.5 and 7.5.

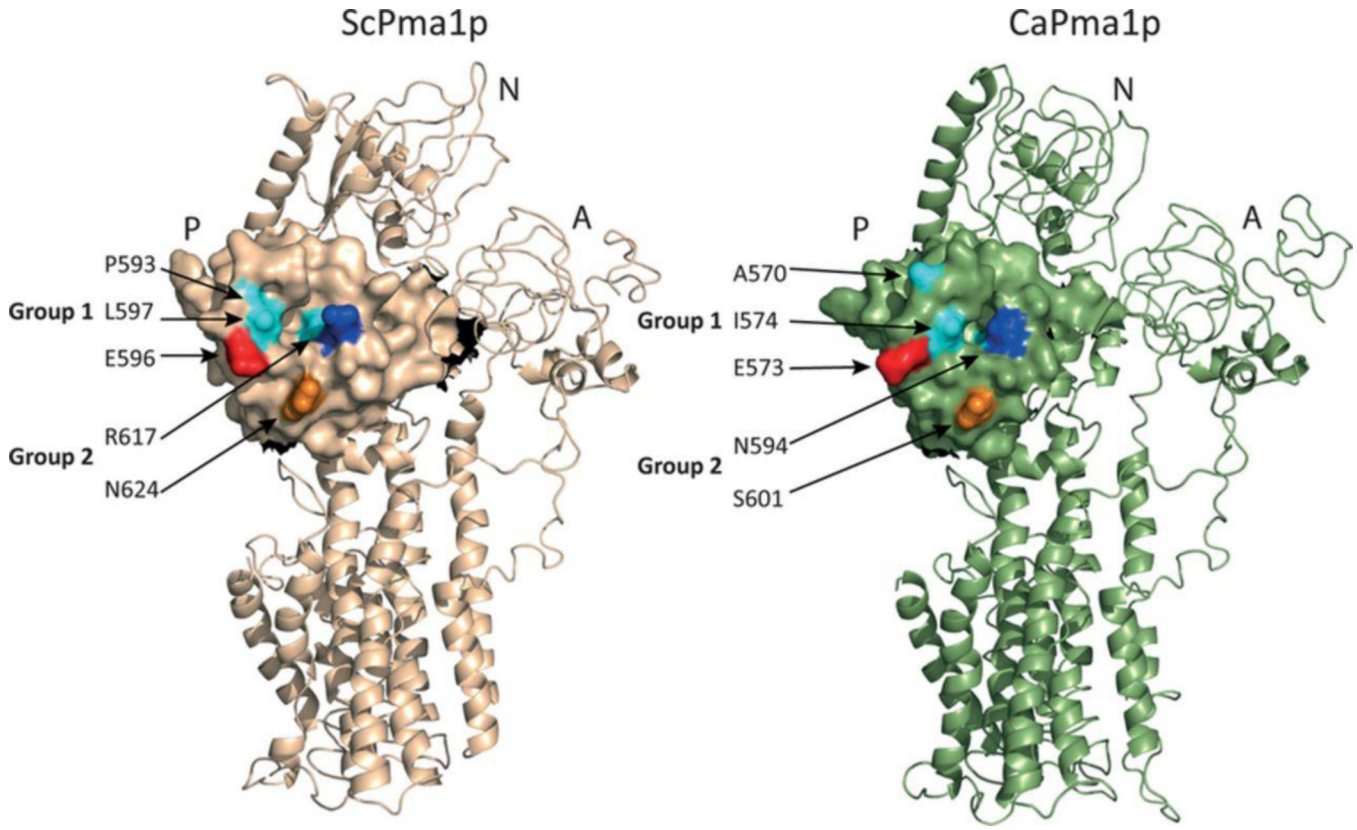

Figure 5.
ScPma1p and CaPma1p homology models based on the Arabidopsis thaliana AHA2 structure.

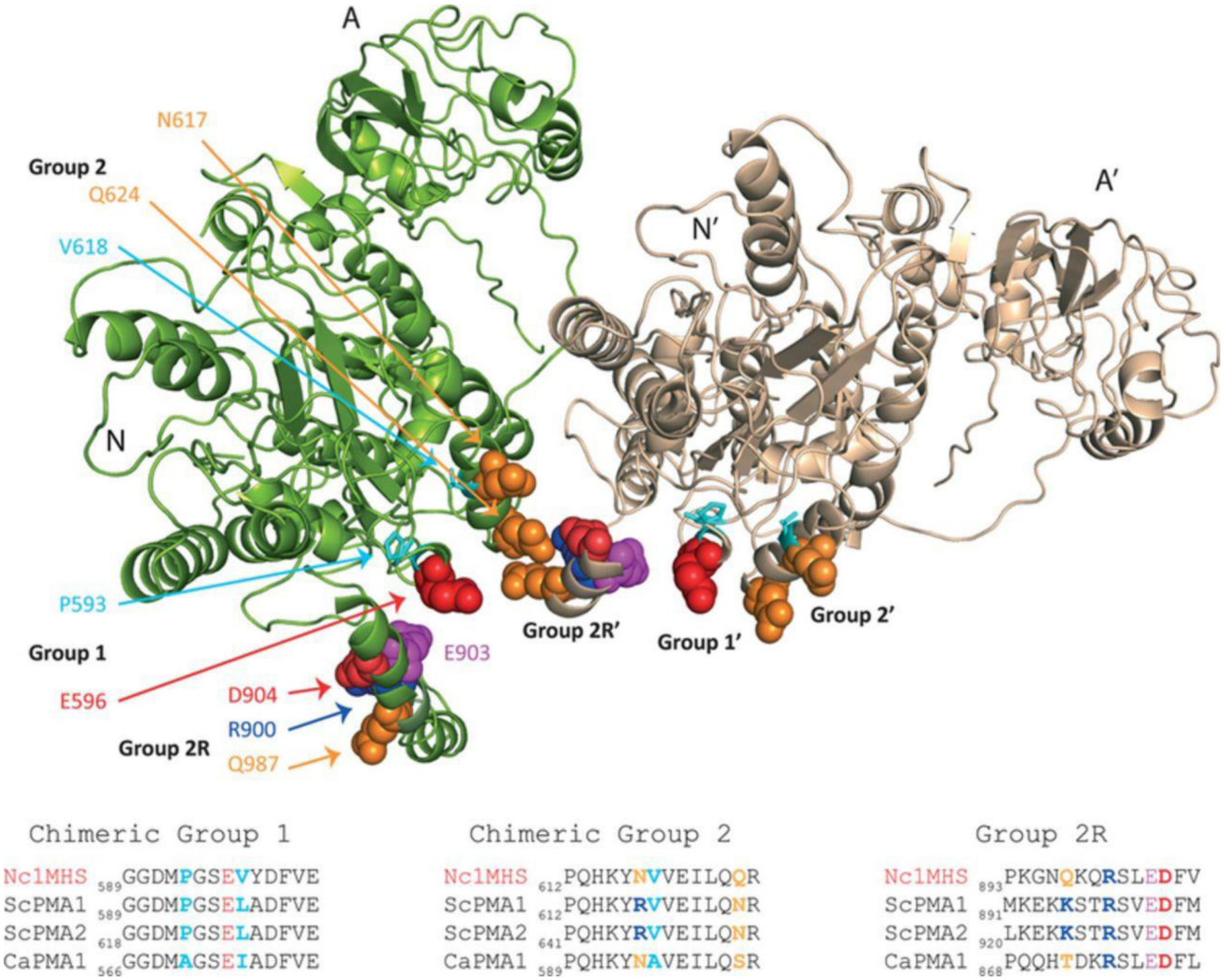

Figure 6.
Neurospora crassa Pma1p (PDB ID: 1mhs) dimer interface.

Table 1

S. cerevisiae strains used in this study.

Strain	Genotype or description	Parent	Source or reference
MMLY663 ADΔ	*MAT a, PDR1-3, his1, Δyor1::hisG, Δsnq2::hisG, Δpdr10::hisG, Δpdr11::hisG, Δycf::hisG, Δpdr3::hisG, Δpdr5::hisG, Δpdr15::hisG, Δura3::200*	AD1-8u$^-$	(Lamping *et al.*, 2005)
MMLY1019	ADΔ, Δ*PMA2*: *kanMX4*	ADΔ	This study
MMLY1020	ADΔ, Δ*PMA1*:*CaPMA1-URA3*	ADΔ	This study
MMLY1022	MMLY1019, Δ*PMA1*:*CaPMA1-URA3*	MMLY1019	This study
MMLY1021	ADΔ, Δ*PMA1*:*CaPMA1*^{a}*-URA3*	MMLY1020	This study
MMLY1087	ADΔ, Δ*PMA1*:*CaPMA1*^{a}*-URA3*	MMLY1020	This study

^{a}chimeric gene, generated spontaneously (see Table 2, Supplementary Fig. S1)

Table 2

Amino-acid substitutions in CaPma1p-ScPma2p chimeric strains

aa in ScPma1p[a] / Strain (Pma)	554	580	582	587	593	597	617	618	624	Protein expression level[b]	Hygromycin B resistance[c]	Acid resistance
ADΔ (ScPma1p)	V_{554}	N_{580}	E_{582}	G_{587}	P_{593}	L_{597}	R_{617}	V_{618}	N_{624}	High	Low 1.0	High
MMLY1022 (CaPma1p)	V_{531}	D_{557}	D_{559}	S_{564}	A_{570}	I_{574}	N_{594}	A_{595}	S_{601}	Low	High 2.9	Low
					Group 1		**Group 2**					
MMLY1021 (chimera)	I_{531}	N_{557}	E_{559}	G_{564}	P_{570}	L_{574}	R_{594}	V_{595}	N_{601}	High	Medium 1.8	High
MMLY1087 (chimera)	V_{531}	D_{557}	D_{559}	S_{564}	P_{570}	L_{574}	R_{594}	V_{595}	N_{601}	High	Low 1.1	High
ADΔ (ScPma2p)[d]	I_{583}	N_{609}	E_{611}	G_{616}	P_{622}	L_{626}	R_{646}	V_{647}	N_{653}			

[a] Amino acid residues that are substituted in the CaPma1p-ScPma1p chimeras are compared by alignment with ScPma1p, ScPma2p and CaPma1p.

[b] The Pma1p expression level was estimated using Coomassie blue-stained SDS PAGE of plasma membrane fractions.

[c] Hygromycin B resistance was expressed as the ratio of the diameters of the zones of inhibition $W_{(AD\ \Delta)}/W_{(strain\ x)}$. Lower resistance results in a larger zone of inhibition and a smaller ratio.

[d] Only I_{583} in ScPma2p is unique to this enzyme.